Toughening of Recycled Poly(Ethylene Terephthalate) with a Maleic Anhydride Grafted SEBS Triblock Copolymer

Zhong-Zhen Yu,[1] Ming-Shu Yang,[1,2] Shao-Cong Dai,[1] Yiu-Wing Mai[1]

[1]*Center for Advanced Materials Technology (CAMT), School of Aerospace, Mechanical and Mechatronic Engineering (J07), The University of Sydney, Sydney, NSW 2006, Australia*
[2]*State Key Laboratory of Engineering Plastics, Center for Molecular Science, Institute of Chemistry, The Chinese Academy of Sciences, P.O. Box 2709, Beijing 100080, China*

Received 10 August 2003; accepted 23 November 2003
DOI 10.1002/app.20592
Published online in Wiley InterScience (www.interscience.wiley.com).

ABSTRACT: Toughening of recycled poly(ethylene terephthalate) (PET) was carried out by blending with a maleic anhydride grafted styrene-ethylene/butylene-styrene triblock copolymer (SEBS-*g*-MA). With 30 wt % of the SEBS-*g*-MA, the notched Izod impact strength of the recycled PET was improved by more than 10-fold. SEM micrographs indicated that cavitation occurred in just a small area near the notch root. Addition of 0.2 phr of a tetrafunctional epoxy monomer increased the recycled PET melt viscosity by chain extension reaction. Different from the positive effect of the epoxy monomer in toughening of nylon and PBT with elastomers, the use of the epoxy monomer in the recycled PET/SEBS-*g*-MA blends failed to further enhance dispersion quality and thus notched impact strength. This negative effect of the epoxy monomer was attributed to the faster reactivity of the epoxy group with maleic anhydride of the SEBS-*g*-MA than with the carboxyl or hydroxyl group of recycled PET. © 2004 Wiley Periodicals, Inc. J Appl Polym Sci 93: 1462–1472, 2004

Key words: recycling; polyethylene terephthalate; impact resistance; compatibilization; reactive extrusion

INTRODUCTION

Poly(ethylene terephthalate) (PET) is a widely used engineering plastic, used especially as soft drink bottles. This market success is mainly caused by its transparency, thermal stability, chemical resistance, and beneficial barrier properties. As a result, fast-growing quantities of used, secondary PET materials become available. The environmental policy of many countries encourages recycling of plastics. As the recycled material after cleaning is unsuitable for production of water or beverage bottles, new approaches for its utilization have to be found. Three recycling methods are of interest, as follows: mechanical recycling including blending and alloying technologies, incineration with energy recovery, and feedstock recycling (pyrolysis, hydrogenation, gasification, chemolysis).[1–7] Of these three methods, mechanical recycling is straightforward and relatively simple. Several attempts were made to recycle PET wastes by mixing with chain extenders to improve their molecular weights and melt viscosities, or by melt blending with other polymers to convert them to high-performance engineering plastics.

Blending of PET with polyolefins and/or elastomers is known to improve certain properties of PET.[8–23] Tanrattanakul et al.[9–12] investigated toughening of PET by blending with maleic anhydride grafted styrene-ethylene/butylenes-styrene triblock copolymer (SEBS-*g*-MA). The *in situ* formation of a graft copolymer by reaction of PET hydroxyl end groups with maleic anhydride was confirmed. The graft copolymer acted as a compatibilizer to lower the interfacial tension and suppress the tendency of coalescence, thus improving the dispersion of SEBS-*g*-MA. Simultaneously, it also enhanced interfacial adhesion between the components.[9] Tensile toughness of the PET was enhanced with 5 wt % SEBS-*g*-MA. Mouzakis et al.[13] studied the static fracture toughness of PET blends with glycidyl methacrylate (GMA)-modified polyolefin elastomer by using the essential work of fracture method. It was found that both essential and nonessential works decreased with increasing elastomer content (up to 20 wt %) if the PET matrix was amorphous and unaged. Heino et al.[19] reported compatibilization of PET/polypropylene (PP) blends with SEBS-*g*-GMA. An addition of 5 wt % of SEBS-*g*-GMA was found to stabilize the blend morphology and improve the impact strength. Lepers et al.[20,21] evaluated the compatibilizing effect of SEBS-*g*-MA in PET/PP blends. Toughening of PET/polycarbonate (PC) blend was studied by adding butylacrylate core-shell elas-

Correspondence to: Z.-Z. Yu (zhongzhen.yu@aeromech.usyd.edu.au).
Contract grant sponsor: Australian Research Council.
Contract grant sponsor: ARC Federation Fellowship.

tomer[22] or ethylene–methacrylate–glycidyl methacrylate copolymer (E-MA-GMA).[23] Studies on toughening mechanisms showed that the major energy dissipating events during impact testing were cavitation and matrix shear yielding.

It is well known that molecular weights of PET are easily reduced during melt processing because of thermal, oxidative, and hydrolytic degradations caused by the simultaneous presence of retained moisture and/or contaminants. Hence, much attention has been to increase the molecular weights (or melt viscosity) and decrease carboxyl content by adding certain chain extenders. Some popular chain extenders are dianhydrides, bis(oxazolines), bis(dihydrooxazines), carbodiimides, diepoxides, and diisocyanates. Thus, Aharoni et al.[24] studied the chain extension reaction of PET with 0.5–2.5 wt % of triphenylphosphite (TPP). Although TPP greatly increased the molecular weight of PET, one drawback was that this reaction also produced diphenylphosphite as byproduct. Inata and Matsumura[25,26] reported chain extension of recycled PET with addition-type heterocyclic bifunctional compounds such as oxazolines, oxazines, or oxazinones. These compounds reacted with the carboxyl or hydroxyl end groups of PET and resulted in chain-extended PET with very low carboxyl content. Cardi et al.[27] confirmed the chain extension effect of 2,2′-bis(2-oxazoline) on recycled PET. Haralabakopoulos et al.[28] showed that some commercially available cyclic diepoxides were effective in chain extension of PET. Xanthos et al.[29] used a diimido-diepoxide compound with low molecular weight and high melting point to reactively modify PET. There was an overall decrease in carboxyl content and increase in hydroxyl content, and intrinsic and melt viscosities. A commercially available tetrafunctional low molecular weight epoxy monomer was also used as chain extender and compatibilizer in PET blends with poly(phenylene ether) (PPE) or thermotropic liquid crystalline polymer (LCP).[30–32]

In a previous work[33,34] by one of us, the influence of 0.3 phr low molecular weight bifunctional epoxy monomer on toughness of nylon 6/maleated polyethylene-octene elastomer (POE-*g*-MA) blend was studied. The bifunctional epoxy monomer was found to play dual roles in the blend. First, the chain extension effect of the epoxy monomer on nylon 6 improved its melt viscosity. Second, the coupling effect of the epoxy monomer at nylon 6/POE-*g*-MA interface resulted in mixed copolymers, which further improved the compatibility of the blend. Both effects combined further enhanced the dispersion of POE-*g*-MA and increased notched impact strengths of nylon 6/POE-*g*-MA blends.[33]

The aim of the present work was to convert recycled PET flakes into polymer materials with high-notched impact strength (toughness) by blending with a commercially available SEBS-*g*-MA. To increase melt viscosity of recycled PET matrix and improve dispersion quality of SEBS-*g*-MA, a tetrafunctional epoxy monomer was added in the recycled PET/SEBS-*g*-MA blends during reactive extrusion. The effectiveness of toughening by SEBS-*g*-MA and the influence of the epoxy monomer were investigated.

EXPERIMENTAL

Materials and processing of blends

Recycled PET flakes were supplied by Coca-Cola Amatil (Australia) and designated r-PET. The number-average and weight-average molecular weights of r-PET measured by GPC were 3.85×10^4 and 11.9×10^4, respectively. Styrene–ethylene/butylene–styrene triblock copolymer grafted with 1.84 wt % of maleic anhydride (SEBS-*g*-MA) was supplied by Shell Chemical Co. (USA) under the trade name of Kraton FG 1901X. It was reported that the ratio of styrene to ethylene/butylene in the triblock copolymer is 28/72 wt % and the glass transition temperature of the SEBS-*g*-MA is −42°C. A tetrafunctional epoxy monomer, *N*,*N*,*N*′,*N*′-tetraglycidyl-4,4′-diaminodiphenyl methane (TGDDM), with epoxy equivalent weight of 110–130 g/eq, was obtained from Ciba-Geigy Pty. Ltd. (The Netherlands).

Before blending, r-PET was dried at 140°C in vacuum for at least 6 h. Blends were prepared in a Werner and Pfleiderer ZSK-30 twin-screw extruder (L/D = 30, L = 0.88 m) at a temperature range of 260–280°C and a screw speed of 330 rpm. The extrudates were pelletized at the die exit, dried, and then injection molded into standard dumbbell tensile (50 mm gauge length, 10 mm width, and 4 mm thickness) and rectangular bars (127 mm length, 12.7 mm width, and 12.7 mm thickness) by an injection-molding machine (SZ-160/80 NB, China), whose barrel temperature was kept at 260°C and the mold was kept at 80°C. The rectangular bars were subsequently cut to two 63.5-mm-long samples for Izod impact testing. A 45° V-notch (depth 2.54 mm) was machined midway on one side of the bar with a slow speed to avoid plastic deformation.

Mechanical testing, viscosity measurements, and morphology observation

Tensile tests were performed on the dumbbell samples in an Instron 5567 testing machine according to ASTM standard D638. Tensile strength, Young's modulus, and elongation-at-break were measured at a crosshead speed of 50 mm/min. Notched Izod impact strength was measured on V-notch bars in a ITR-2000 instrumented impact tester by using ASTM standard D256. During impact testing, a load cell in the tup recorded the force generated in the deformed sample. Assuming the hammer did not change speed greatly during

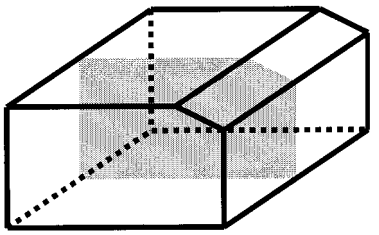

Figure 1 The location of fracture flank in gray color produced by cryofracturing of the Izod impact specimen for SEM observation.

fracture due to energy absorbed by the sample and effect of gravity, the load-deflection curve was obtained. The integral of the load-deflection curve gave the fracture energy absorbed. Except where indicated, all these tests were conducted at ambient temperature (~ 20–25°C) and the average value of five repeated tests was taken for each composition.

Dynamic viscosity measurements were conducted on a Rheometer Bohlin VOR-HTC with 25-mm-diameter parallel plates at 280°C under protection in nitrogen atmosphere. The gap between the plates was 1.0 mm. The specimens were predried in a vacuum oven at 100°C for 6 h. Each specimen was first heated to 280°C and held at that temperature until thermal equilibrium was established between the plate and the melt. The temperature was measured by using a thermocouple located in the center of the top plate.

To evaluate fracture mechanisms, the fracture surface as well as the fracture flank of impact specimens were coated with gold and then observed with a Philips S-505 scanning electron microscope (SEM). The fracture flank in a plane perpendicular to the fracture surface and parallel to the crack propagation direction, shown in Figure 1, was cut from the impact-tested specimen under liquid nitrogen temperature. A notch was introduced before cryofracturing so as to get a smooth surface. To assess the dispersion quality of SEBS-*g*-MA, image analysis was carried out to measure the apparent diameter (a_i) of the dispersed phase, which was then converted into true particle diameter (d_i).[35] Typically, over 200 particles from different photographs of a specimen surface were analyzed to calculate the number-average diameter d_n from the following relationship:

$$\bar{d}_n = \sum n_i d_i \Big/ \sum n_i \quad (1)$$

where n_i is the number of particles having the true particle diameter d_i.

RESULTS AND DISCUSSION

Dispersion of SEBS-*g*-MA

To assess the dispersion quality of SEBS-*g*-MA in recycled PET, Figure 2 displays SEM micrographs of fracture surfaces of r-PET/SEBS-*g*-MA blends. The SEBS-*g*-MA particles are fine and homogeneous. Figure 3 presents the effects of SEBS-*g*-MA content on number-average diameter of dispersed phase in recycled PET matrix. The average diameter of SEBS-*g*-MA is very similar, ranging from 0.89 to 0.98 μm, irrespective of its contents, which is a direct characteristic of a compatibilized blend. The compatibility between r-PET and SEBS-*g*-MA is derived from the PET-*co*-SEBS-*g*-MA copolymer formed *in situ* during melt extrusion:[9]

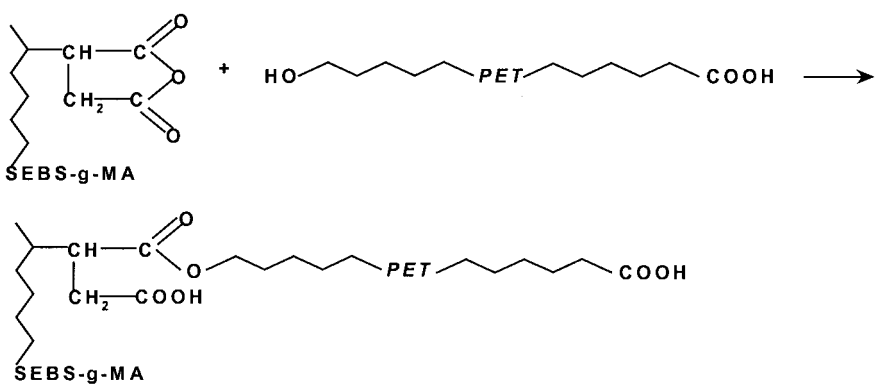

Tanrattanakul et al.[9] confirmed this chemical reaction. In their work, blends of PET with grafted SEBS-*g*-MA and nongrafted SEBS were extracted by tetrahydrofuran (THF) to isolate an SEBS-*g*-MA component that had chemically reacted with PET. THF is a good solvent for SEBS and SEBS-*g*-MA, but is a nonsolvent for PET. The THF-insoluble fraction was characterized by photoacoustic FTIR. They showed that most of the SEBS-*g*-MA did not react with PET and thus was extracted with THF; only a small amount reacted with PET because of the weak reactivity between hydroxyl and anhydride groups.

Mechanical properties

Figure 4 shows notched Izod impact strengths plotted as a function of SEBS-*g*-MA content for r-PET/SEBS-

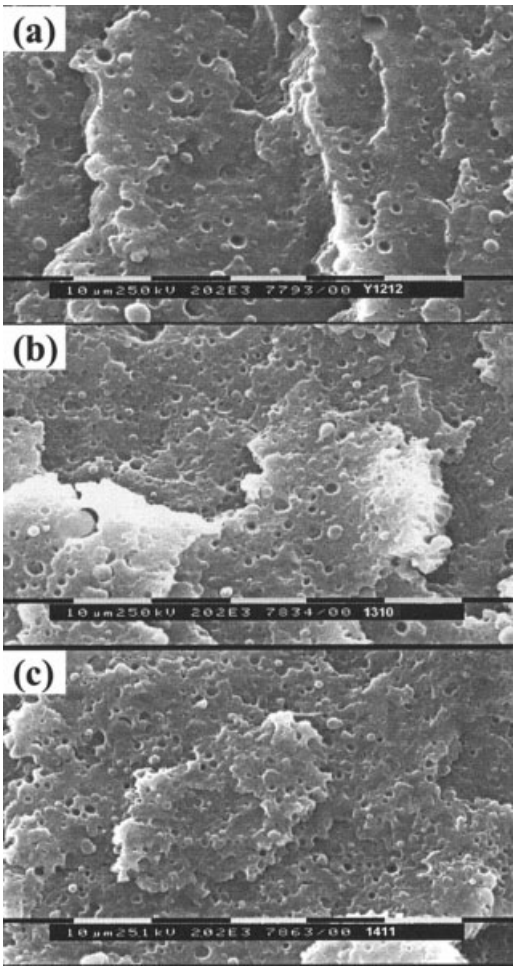

Figure 2 High-magnification SEM micrographs of impact-fractured surfaces of r-PET blends with SEBS-*g*-MA contents of (a) 10 wt %, (b) 20 wt %, and (c) 30 wt %, respectively, showing the sizes of the elastomers.

g-MA blends with and without 0.2 phr of the tetrafunctional epoxy monomer. The recycled PET has low-notched impact strength, about 10.5 J/m at ambient temperature. Addition of 30 wt % SEBS-*g*-MA increases the notched impact strength of recycled PET by more than 10-fold. Even though SEBS-*g*-MA was effective in toughening recycled PET flakes, its efficiency is much less than that in toughening nylon and poly(butylene terephthalate) (PBT).[36–38] In addition, 0.2 phr of the epoxy monomer only increases slightly the notched impact strength of the recycled PET because of its chain extension effect on r-PET. Surprisingly, when 0.2 phr epoxy monomer was added to the r-PET/SEBS-*g*-MA during melt extrusion, the notched impact strengths of the blends are not improved but reduced. The negative effect of the epoxy monomer will be explained later.

Figure 5 depicts typical stress–strain curves of r-PET and its blends with different SEBS-*g*-MA contents. Tensile properties such as Young's modulus, yield strength, fracture strength, and elongation at break are listed in Table I. As a semicrystalline polymer, PET normally has good ductility.[9–12] However, r-PET broke before yielding. It should be noted that, when r-PET was injection molded, the mold temperature was kept at 80°C to obtain a specimen with low shrinkage and good dimension stability. The high mold temperature favored increases of crystallization rate and crystallinity and thus lowered the ductility of the recycled PET. Also, impurities in r-PET could cause degradation during melt extrusion and subsequent injection molding and thus impair its ductility.[6] Except for the pristine r-PET, all the blends showed yielding followed by necking. The engineering stress

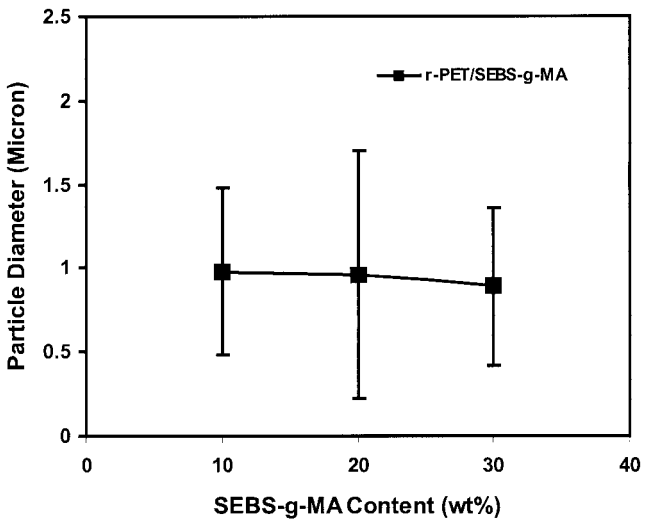

Figure 3 Plot of number-average diameter against SEBS-*g*-MA content for r-PET/SEBS-*g*-MA blends.

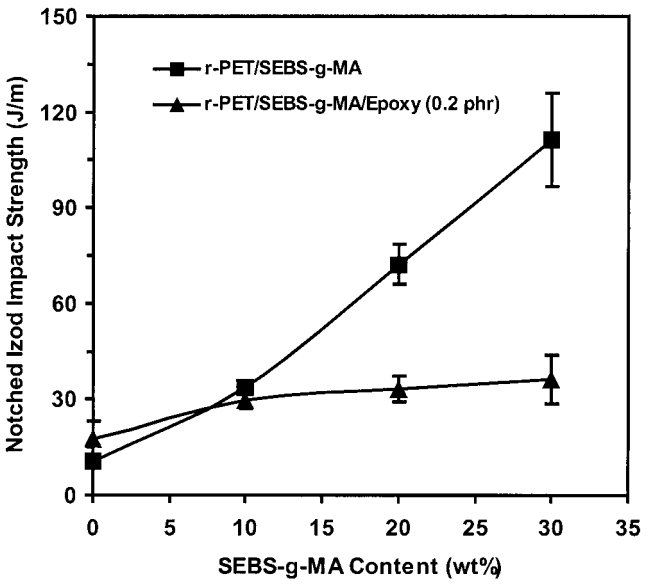

Figure 4 Plots of notched Izod impact strength as a function of SEBS-*g*-MA content for r-PET/SEBS-*g*-MA blends with and without the tetrafunctional epoxy monomer.

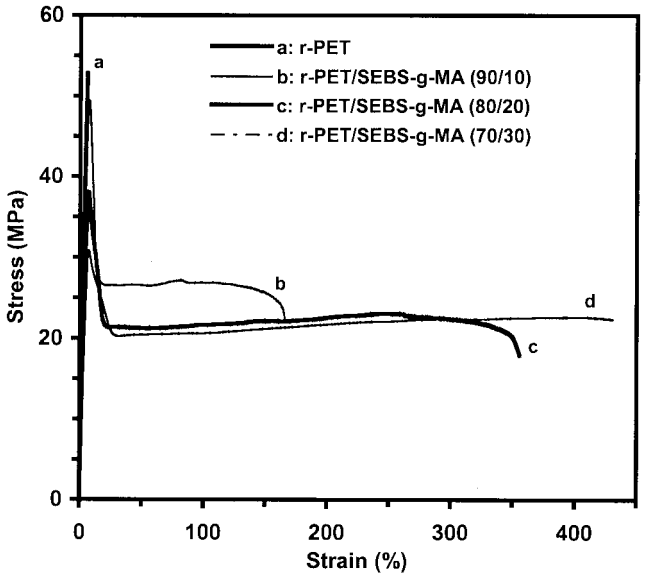

Figure 5 Typical stress–strain curves of r-PET and its blends with different SEBS-*g*-MA contents at a speed of 50 mm/min.

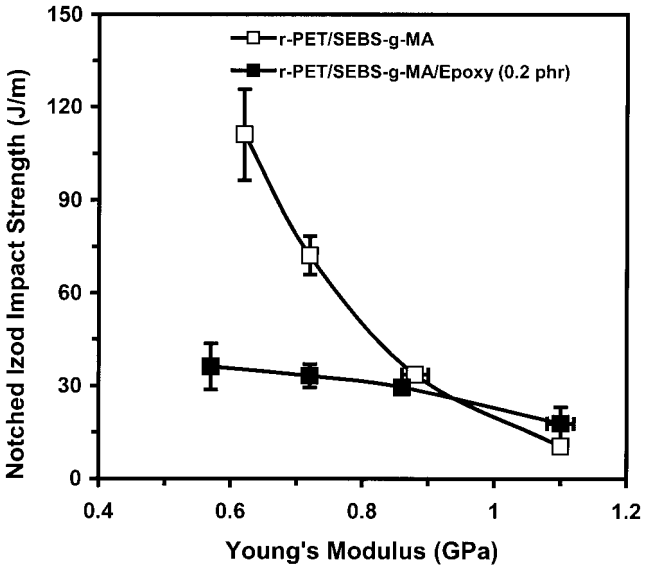

Figure 6 Plots of notched Izod impact strength against Young's modulus for r-PET/SEBS-*g*-MA blends with or without the tetrafunctional epoxy monomer.

increased with engineering strain and reached a maximum at yield point, corresponding to formation of a neck in the specimen width. Post yielding, the engineering stress rapidly dropped to about half the yield stress as necking started to spread to the end of the gauge section. During necking, the stress was constant. Most of the r-PET/SEBS-*g*-MA specimens fractured during necking. However, few r-PET/SEBS-*g*-MA (70/30) specimens did not break after necking spread to both ends of the gauge section, and thereafter, the necked down region appeared to be strain-hardened under increasing stress. In this circumstance, tests were discontinued without specimen failure. Hence, no fracture strengths are given for the r-PET blends.

Careful inspections of the elongation at break data for the r-PET/SEBS-*g*-MA blends reported in Table I indicate that the addition of SEBS-*g*-MA has a large improvement on elongation of r-PET but little influence on that of r-PET with 0.2 phr epoxy monomer. This relative effect of the epoxy monomer disappears when the Young's modulus data are examined closely. Indeed, Young's moduli for r-PET/SEBS-*g*-MA blends with or without the epoxy monomer decrease almost linearly with SEBS-*g*-MA content, a trend that is expected of elastomer toughened polymers.

Toughness and stiffness are two important properties for a structural material. To clearly evaluate the effects of the epoxy monomer on toughness and modulus, Figure 6 shows plots of notched Izod impact strength against Young's modulus for r-PET/SEBS-*g*-MA blends with and without 0.2 phr epoxy monomer. It was thought that addition of the epoxy monomer would move the PET/SEBS-*g*-MA blends upward to the zone with high-notched impact strength and high stiffness. In fact, the resultant effect of the epoxy monomer was negative, evidenced by reductions in notched impact strength (toughness), Young's modulus (stiffness), and elongation to break (ductility). These results are at odds with results obtained in

TABLE I
Tensile Properties of r-PET and Its Blends with or without 0.2 phr Tetrafunctional Epoxy Monomer Measured at Crosshead Speed of 50 mm/min

Composition	Elongation at break (%)	Young's modulus (GPa)	Yield strength (MPa)	Break strength (MPa)
r-PET	6 ± 1	1.10 ± 0.01	—	65.4 ± 4.6
r-PET/SEBS-*g*-MA (90/10)	160 ± 10	0.88 ± 0.02	48.3 ± 0.9	—
r-PET/SEBS-*g*-MA (80/20)	346 ± 34	0.72 ± 0.01	38.4 ± 0.6	—
r-PET/SEBS-*g*-MA (70/30)	433 ± 153	0.62 ± 0.01	31.2 ± 0.9	—
r-PET/Epoxy (100/0.2)	41 ± 26	1.10 ± 0.02	65.0 ± 1.3	—
r-PET/SEBS-*g*-MA/Epoxy (90/10/0.2)	108 ± 29	0.86 ± 0.01	46.2 ± 1.1	—
r-PET/SEBS-*g*-MA/Epoxy (80/20/0.2)	56 ± 6	0.72 ± 0.01	37.1 ± 0.98	—
r-PET/SEBS-*g*-MA/Epoxy (70/30/0.2)	92 ± 20	0.57 ± 0.01	28.4 ± 0.92	—

nylon 6/POE-*g*-MA blends and PBT/E-MA-GMA blends,[33,34,36] for which small amounts of epoxy monomers showed positive effects on toughness and stiffness of the blends. Figure 7 displays notched Izod impact strength versus flexural modulus for nylon 6/POE-*g*-MA blends with or without 0.3 phr of a bifunctional diglycidyl ether of bisphenol-A (DGEBA) epoxy monomer.[33] For required notched impact strength, it is seen that the blend with the DGEBA epoxy monomer has higher flexural modulus than the blend without DGEBA epoxy monomer. Likewise, for a required flexural modulus, the blend with DGEBA monomer shows higher notched impact strength than the blend without the monomer. Similarly, Figure 8 indicates that the additions of a tetrafunctional epoxy monomer into PBT/E-MA-GMA blends have the same effect of increasing both notched impact strength and stiffness relative to the blends without the monomer.[36]

Fractography

To elucidate the effects of SEBS-*g*-MA and epoxy monomer on notched impact strength, we need to study the impact-fracture surfaces of the recycled PET and its blends. Figure 9 presents SEM micrographs for r-PET, which display two regions: one for slow growth initiated at the notch root followed by another for subsequent fast crack growth, Figure 9(a). The slow growth region exhibits a smooth, featureless surface, even under a high magnification, Figure 9(b). When the crack reached its critical length, it became unstable and spread rapidly, giving a nonplanar crack growth, Figure 9(c).

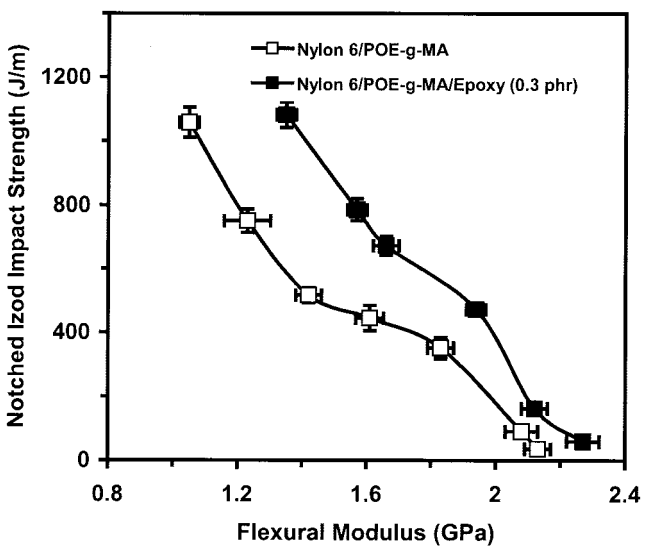

Figure 7 Plots of notched Izod impact strength against flexural modulus for nylon 6/POE-*g*-MA blends with or without a bifunctional diglycidyl ether of bisphenol-A (DGEBA) epoxy monomer.[33]

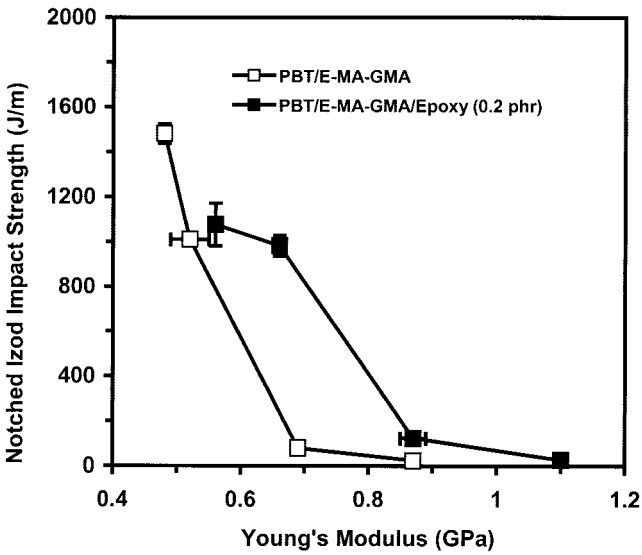

Figure 8 Plots of notched Izod impact strength against Young's modulus for PBT/E-MA-GMA blends with or without the tetrafunctional epoxy monomer.[36]

Figure 10 displays SEM micrographs of impact-fracture surfaces of the recycled PET blended with 10 wt % of SEBS-*g*-MA. Cavitation is clearly seen in the slow crack growth region adjacent to the V-notch root, Figure 10(a, c), which is thought to be largely responsible for the enhanced impact strength of the blend. The fast nonplanar crack growth, Figure 10(d), exhibits no cavitation even though the SEBS-*g*-MA particles are homogeneously dispersed. It is also noted that many nonspherical but elongated SEBS-*g*-MA particles exist in regions near the lateral surfaces of the injection-molded specimen, Figure 10(b). During the injection-molding process, the melt in the neighborhood of the wall of the mold experienced strong shearing stresses, so that the SEBS-*g*-MA particles were elongated to platelets parallel to the wall. Away from the wall, the shearing stresses decreased and the SEBS-*g*-MA dispersed phase converted back to stable spherical shapes. The thickness of this elongation region is not larger than 1 mm. Tanrattanakul et al.[10] characterized the elongation of SEBS-*g*-MA in PET by examining the edge and bulk of injection-molded samples that were freeze-fractured parallel and normal to injection direction and then etched to remove the SEBS-*g*-MA phase. It was found that the elastomers near the edge were platelet-shaped, whereas those in the bulk were spherical and had the same size as the extruded pellets. It should be pointed out that the presence of the elongation zone does not affect the notched impact strength values because the V-notch introduced in the samples is 2.54 mm in depth.

Similar observations are seen in the SEM micrographs in Figures 11 and 12 for the recycled PET blends with 20 and 30 wt % of SEBS-*g*-MA. In the slow crack growth region, Figures 11(b) and 12(b), cavita-

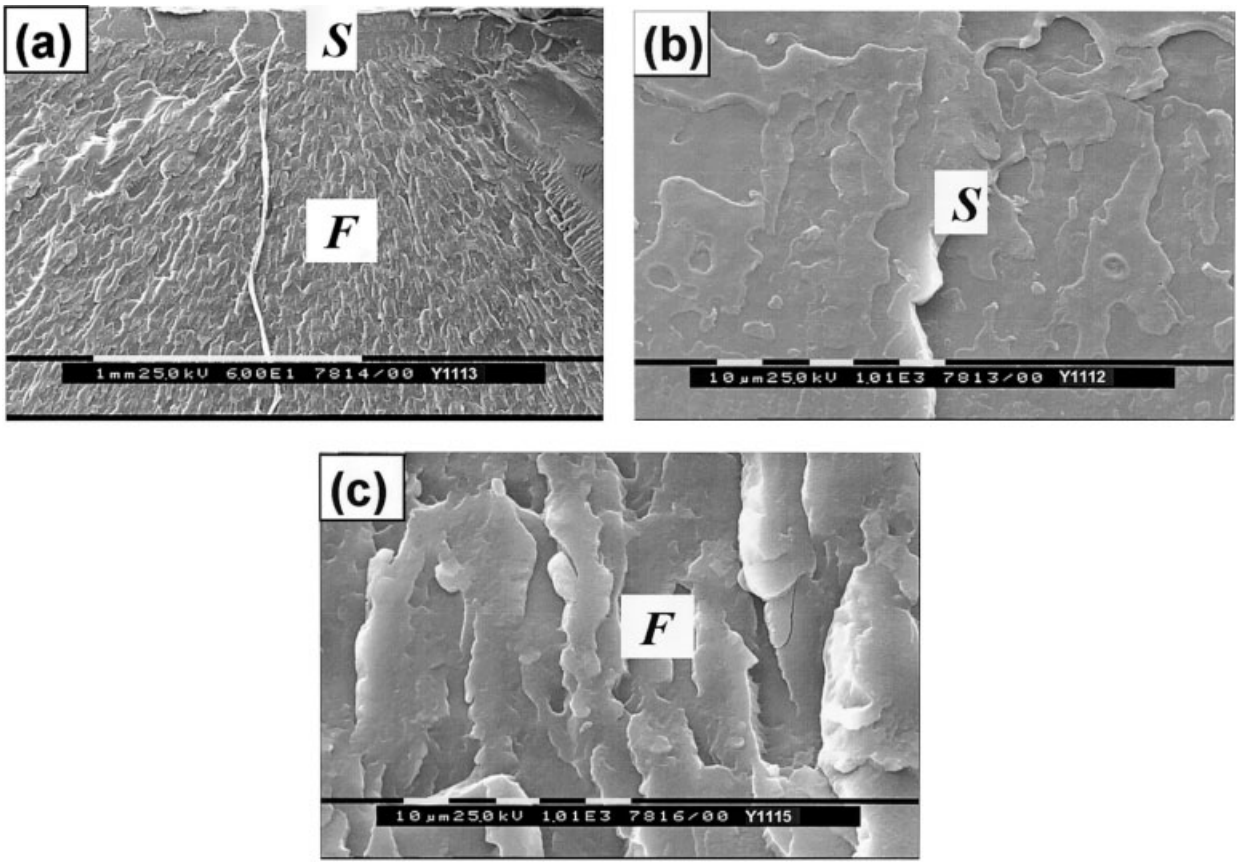

Figure 9 Low (a) and high (b, c) magnification SEM micrographs of impact-fractured surfaces of r-PET showing characteristics of the slow *S* and *F* crack growth regions.

tion is more extensive compared to that observed in the r-PET/SEBS-*g*-MA (90/10) blend [Fig. 10(c)]. Nonplanar growth is again noticeable in the fast growth region, Figures 11(a) and 12(a). It appears that the notch impact strength of these blends increases with the size of the slow crack growth region where the

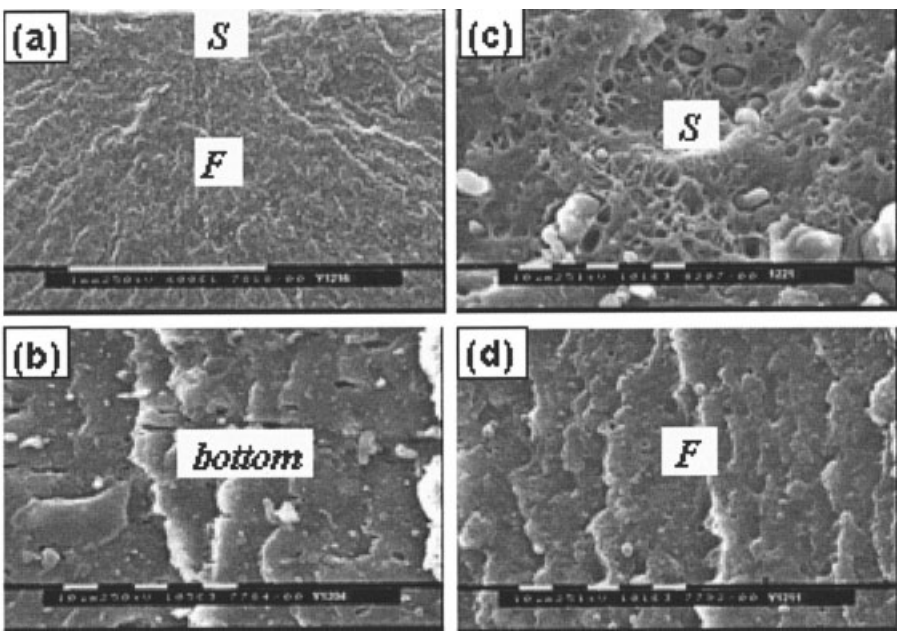

Figure 10 Low (a, b) and high (c, d) magnification SEM micrographs of impact-fractured surface of r-PET/SEBS-*g*-MA (90/10) blend. *S* and *F* denote slow and fast crack growth regions, respectively.

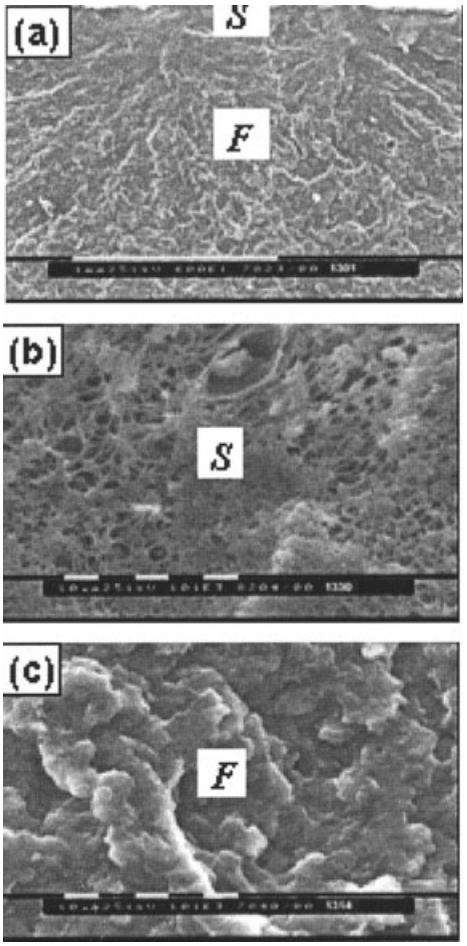

Figure 11 Low (a) and high (b, c) magnification SEM micrographs of impact-fractured surface of r-PET/SEBS-*g*-MA (80/20) blend showing slow *S* and fast *F* crack growth regions.

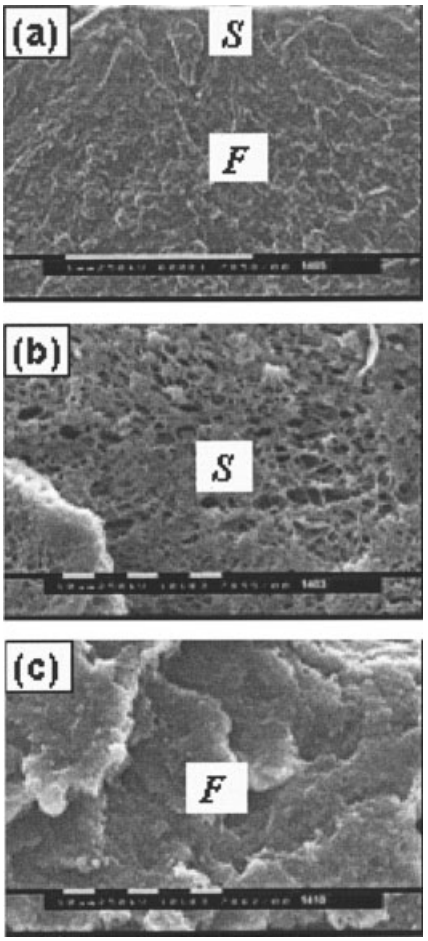

Figure 12 Low (a) and high (b, c) magnification SEM micrographs of impact-fractured surface of r-PET/SEBS-*g*-MA (70/30) blend showing slow *S* and fast *F* crack growth regions.

extent of cavitation depends on the elastomer content. It should be noted that the stress-whitening zone cannot be observed in the fracture flank near the impact-fractured surface even if the content of SEBS-*g*-MA is up to 30 wt %. Figure 13 displays a SEM photograph of the fracture flank near the fracture surface of the r-PET/SEBS-*g*-MA (70/30) blend. The fracture surface is located at the top. It is clear that no cavitation and matrix yielding are observed under the impact-fractured surface. The recycled PET blend displays a brittle fracture, although its notched Izod impact strength is improved by more than 10-fold with 30 wt % of SEBS-*g*-MA. However, 20–30 wt % of MA- or GMA-grafted elastomers was enough to supertoughen nylon and PBT thermoplastics, evidenced by over 20-fold increase of notched impact strength caused by extensive cavitation and matrix shear yielding.[33–39]

To obtain a supertoughened PET, the elastomer component should have finer dispersion by further improving its compatibility with PET. For this purpose, a tetrafunctional epoxy monomer was used in the r-PET/SEBS-*g*-MA blends in this work. Figures 14-16 depict SEM micrographs of impact-fractured surfaces of these recycled blends with 0.2 phr epoxy monomer. It is surprising that the dispersion quality

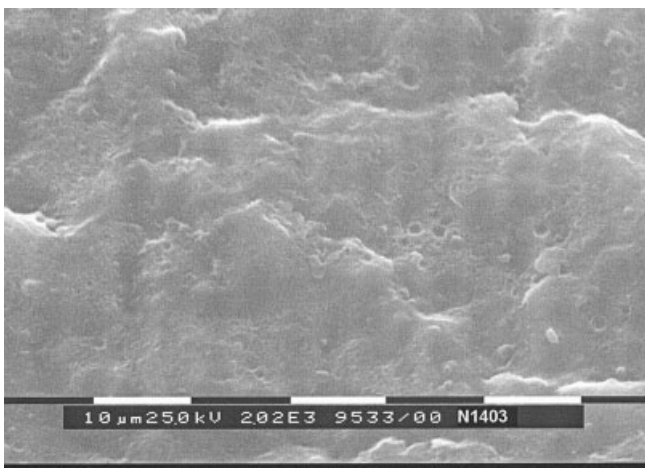

Figure 13 SEM micrographs of fracture flank perpendicular to impact-fractured surface and parallel to crack propagation direction of r-PET/SEBS-*g*-MA (70/30) blend.

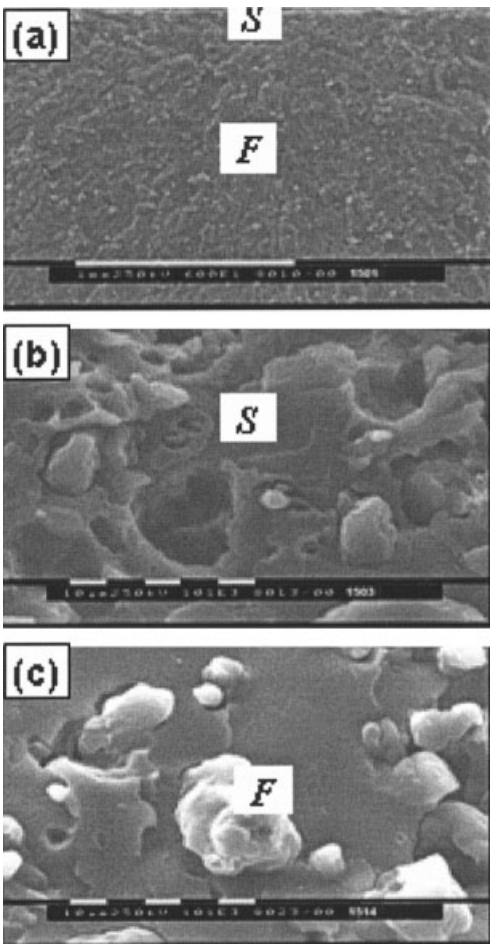

Figure 14 Low (a) and high (b, c) magnification SEM micrographs of impact-fractured surfaces of r-PET/SEBS-*g*-MA (90/10) blends with 0.2 phr of tetrafunctional epoxy monomer. *S* and *F* denote slow and fast crack growth regions, respectively.

of SEBS-*g*-MA was not improved. In fact, dispersion becomes worse, and the SEBS-*g*-MA particles are very large and could be visible under a low magnification, Figures 14(a), 15(a), and 16(a). No cavitation appeared in both the slow and the fast crack growth regions, Figures 14(b, c), 15(b, c), and 16(b, c).

The negative effect of the epoxy monomer on dispersion of SEBS-*g*-MA can be understood by considering the competitive reactions among SEBS-*g*-MA, r-PET, and epoxy monomer. In the r-PET/SEBS-*g*-MA two-component blends, SEBS-*g*-MA reacted with the hydroxyl group of r-PET, forming a copolymer *in situ*, which is responsible for the uniform dispersion of SEBS-*g*-MA in r-PET. Similarly, with use of epoxy monomer in r-PET, the epoxy group reacted with the carboxyl and hydroxyl groups in the melt, thus increasing the molecular weights of r-PET as confirmed by an increase in viscosity, Figure 17. This is responsible for enhanced mechanical properties of r-PET. Conversely, the situation was changed when the epoxy monomer was added as a third component to the r-PET/SEBS-*g*-MA components during melt extrusion. Because the reactivity between epoxy and anhydride groups is higher than that between epoxy and carboxyl/hydroxyl groups and that between hydroxyl and anhydride groups, the epoxy monomer preferentially reacted with maleic anhydride groups of SEBS-*g*-MA than with the groups of r-PET. The preferential reaction increased viscosity of the SEBS-*g*-MA rather than that of the matrix and enlarged the viscosity mismatch between the recycled PET and SEBS-*g*-MA adversely affecting the dispersion of the SEBS-*g*-MA. Besides, this preferential reaction consumed most of maleic anhydride groups on SEBS-*g*-MA, so that r-PET did not have an opportunity to form a copolymer with SEBS-*g*-MA. This was another factor not favoring dispersion of SEBS-*g*-MA. Also, it is reasonable to speculate that the increased viscosity of r-PET/SEBS-*g*-MA (80/20) blend due to the use of the epoxy monomer, as shown in Figure 17, is caused mainly by the viscosity increase of the SEBS-*g*-MA dispersed phase.

It can be seen that the size of SEBS-*g*-MA shows a trend to decrease with increasing SEBS-*g*-MA con-

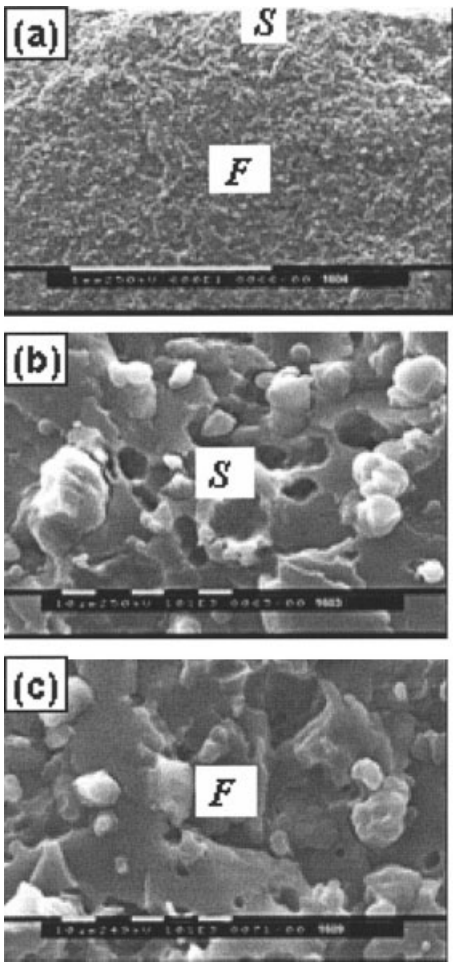

Figure 15 Low (a) and high (b, c) magnification SEM micrographs of impact-fractured surfaces of r-PET/SEBS-*g*-MA (80/20) blends with 0.2 phr of tetrafunctional epoxy monomer. *S* and *F* denote slow and fast crack growth regions, respectively.

tents. This can also be explained by the competitive reactions in the three-component blend. At low SEBS-*g*-MA content, the maleic anhydride groups are mainly consumed by the epoxy monomer, resulting in the worst dispersion of these particles. With high SEBS-*g*-MA content, not all anhydrides are taken up by the epoxy monomer; some react with hydroxyl groups of r-PET to generate a PET-*co*-SEBS-*g*-MA copolymer, which benefits dispersion of the SEBS-*g*-MA.

Generally, to obtain a fine dispersion of a dispersed phase (*D*) in a thermoplastic matrix (*M*) by adding a small amount of reactive component (*R*), the reaction rates among them should be $(R - M) \geq (R - D)$. For example, in nylon 6/POE-*g*-MA/epoxy monomer (0.3 phr) blends, because the epoxy group reacts faster with the amine end group of nylon 6 than with the maleic anhydride group of POE-*g*-MA, the use of epoxy monomer increases the matrix viscosity by chain extension reaction with nylon 6; at the same time, it generates a nylon 6-*co*-epoxy-*co*-POE-*g*-MA copolymer by a coupling reaction at the interface between nylon 6 and POE-*g*-MA, resulting in a fine dispersion and thus improves toughening efficiency of POE-*g*-MA.[33] Similarly, as shown in Figure 8, the positive effects of the epoxy monomer on notched impact strength and stiffness of the PBT/SEBS-*g*-MA/epoxy blends can be attributed to the comparable reactivity of the epoxy group of the monomer with the carboxyl group of the PBT and the epoxy group of the elastomer.[36] Chiou and Chang[40] reported reactive compatibilization of nylon 6/PBT blends with 0.3 phr of the tetrafunctional epoxy monomer. As the epoxy group reacted faster with amine group of nylon 6 than with carboxyl group of PBT, this explained why compatibilization of epoxy monomer was more effective in nylon 6 rich than PBT-rich blends. The positive compatibilization of the tetrafunctional epoxy monomer on PET/PPE (70/30) blends was also caused by the faster reaction of epoxy with PET than with PPE.[30]

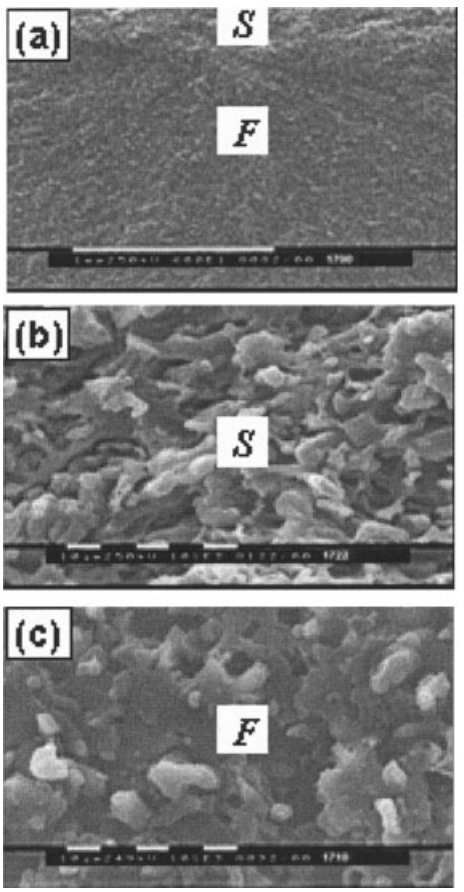

Figure 16 Low (a) and high (b, c) magnification SEM micrographs of impact-fractured surfaces of r-PET/SEBS-*g*-MA (70/30) blends with 0.2 phr of tetrafunctional epoxy monomer. *S* and *F* denote slow and fast crack growth regions, respectively.

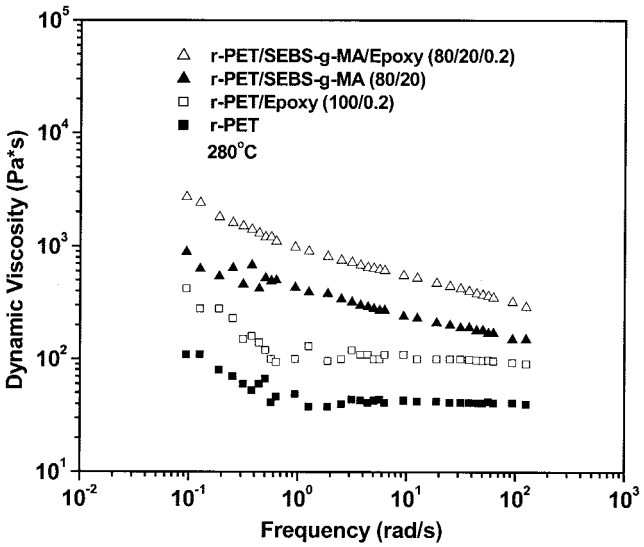

Figure 17 Plots of dynamic viscosity against frequency for r-PET and r-PET/SEBS-*g*-MA (80/20) blends with and without 0.2 phr of tetrafunctional epoxy monomer at 280°C

CONCLUSION

SEBS-*g*-MA elastomer was effective in toughening recycled PET. The elastomer (30 wt %) was found to increase the notched Izod impact strength of r-PET by more than 10-fold. SEM micrographs indicated that cavitation occurred in a small area ahead of the notch root but no matrix shear yielding was found. SEBS-*g*-MA was homogeneously dispersed in the recycled PET matrix but the sizes were relatively large, ~ 0.89 –0.98 μm. To obtain a supertough blend, a much finer dispersion is needed.

With 0.2 phr of a tetrafunctional epoxy monomer blended with r-PET, their mechanical properties were slightly improved because of the chain extension reaction of the monomer. Different from the positive effect of the epoxy monomer in toughening of nylon

and PBT with maleated or GMA-grafted elastomers, the use of epoxy monomer in the recycled PET/SEBS-*g*-MA blends failed to further improve the notched impact strength. SEM micrographs confirmed that the dispersion of SEBS-*g*-MA became worse upon adding the epoxy monomer. By considering the competitive reactions among SEBS-*g*-MA, r-PET, and epoxy monomer, this negative effect of the epoxy monomer on dispersion of SEBS-*g*-MA should be attributed to the faster reactivity of the epoxy group with maleic anhydride groups of the SEBS-*g*-MA than with the carboxyl and hydroxyl groups of the recycled PET matrix.

The authors thank the Australian Research Council (ARC) for the continuing support of this project on "Rubber Toughening of Recycled PET." Y.-W. Mai also acknowledges the award of an ARC Federation Fellowship tenable at the University of Sydney.

References

1. La Mantia, F. P.; Vinci, M. Polym Degrad Stab 1994, 45, 121.
2. Tsiourvas, D.; Tsartolia, E.; Stassinopoulos, A.; Barrell, M.; Bontemps, J. Adv Polym Tech 1995, 14, 227.
3. Martínez, J. M.; Eguiazábal, J. I.; Nazábal, J. J Macromol Sci Phys 1995, B34 (1&2), 171–176.
4. Milana, M. R.; Denaro, M.; Arrivabene, L.; Maggio, A.; Gramiccioni, L. Food Addit Contam 1998, 15, 355.
5. Paci, M.; La Mantia, F. P. Polym Degrad Stab 1998, 61, 417.
6. Torres, N.; Robin, J. J.; Boutevin, B. Eur Polym J 2000, 36 2075.
7. Billiau, M.; Durand, G.; Tersac, G. Polymer 2002, 43, 21.
8. Young M. W.; Xanthos, M.; Biesenberger, J. A. Polym Eng Sci 1990, 30, 355.
9. Tanrattanakul, V.; Hiltner, A.; Baer, E.; Perkins, W. G.; Massey, F. L. Polymer 1997, 38, 2191.
10. Tanrattanakul, V.; Hiltner, A.; Baer, E.; Perkins, W. G.; Massey, F. L. Polymer 1997, 38, 4117.
11. Pawlak, A.; Perkins, W. G.; Massey, F. L.; Hiltner, A.; Baer, E. J Appl Polym Sci 1999, 73, 203.
12. Tanrattanakul, V.; Perkins, W. G.; Massey, F. L.; Moet, A.; Hiltner, A.; Baer, E. J Mater Sci 1997, 32, 4749.
13. Mouzakis, D. E.; Papke, N.; Wu, J. S.; Karger-Kocsis, J. J Appl Polym Sci 2001, 79, 842.
14. Kalfoglou, N. K.; Skafidas, D. S.; Kallitsis, J. K. Polymer 1996, 37, 3387.
15. Papke, N.; Karger-Kocsis, J. Polymer 2001, 42, 1109.
16. Papadopoulou, C. P.; Kalfoglou, N. K. Polymer 2000, 41, 2543.
17. Torres, N.; Robin, J. J.; Boutevin, B. J Appl Polym Sci 2001, 81, 2377.
18. Lusinchi, J. M.; Boutevin, B.; Torres, N.; Robin, J. J. J Appl Polym Sci 2001, 79, 874.
19. Heino, M.; Kirjava, J.; Hietaoja, P.; Seppälä, J. J Appl Polym Sci 1997, 65, 241.
20. Lepers, J. C.; Favis, B. D.; Lacroix, C. J Polym Sci, Part B: Polym Phys 1999, 37, 939.
21. Lepers, J. C.; Favis, B. D.; Tabar, R. J. J Polym Sci, Part B: Polym Phys 1997, 35, 2271.
22. Liao, Z. L.; Chang, F. C. J Appl Polym Sci 1994, 52, 1115.
23. Wu, J. S.; Xue, P.; Mai, Y. W. Polym Eng Sci 2000, 40, 786.
24. Aharoni, S. M.; Forbes, C. E.; Hammond, W. B.; Hindenlang, D. M.; Mares, F.; O'brien, K.; Sedgwick, R. D. J Polym Sci, Part B: Polym Chem 1986, 24, 1281.
25. Inata, H.; Matsumura, S. J Appl Polym Sci 1986, 32, 4581.
26. Inata, H.; Matsumura, S. J Appl Polym Sci 1987, 33, 3069.
27. Cardi, N.; Po, R.; Giannotta, G.; Occhiello, E.; Garbassi, F.; Messina, G. J Appl Polym Sci 1993, 50, 1501.
28. Haralabakopoulos, A. A.; Tsiourvas, D.; Paleos, C. M. J Appl Polym Sci 1999, 71, 2121.
29. Xanthos, M.; Young, M. W.; Karayannidis, G. P.; Bikiaris, D. N. Polym Eng Sci 2001, 41, 643.
30. Lo, D. W.; Chiang, C. R.; Chang, F. C. J Appl Polym Sci 1997, 65, 739.
31. Chin, H. C.; Chang, F. C. Polymer 1997, 38, 2947.
32. Qiao, F.; Migler, K. B.; Hunston, D. L.; Han, C. C. Polym Eng Sci 2001, 41, 77.
33. Yu, Z. Z.; Ou, Y. C.; Hu, G. H. J Appl Polym Sci 1998, 69, 1711.
34. Yu, Z. Z.; Ou, Y. C.; Qi, Z. N.; Hu, G. H. J Polym Sci, Part B: Polym Phys 1998, 36 1987.
35. Wu, S. Polymer 1985, 26, 1855.
36. Yu, Z. Z.; Yan, C.; Ma, J.; Dai, S. C.; Yang, M. S.; Mai, Y. W. Macromol Mat Eng, to appear.
37. Oshinski, A. J.; Keskkula, H.; Paul, D. R. Polymer 1996, 37, 4909.
38. Kayano, Y.; Keskkula, H.; Paul, D. R. Polymer 1998, 39, 2835.
39. Arostegui, A.; Gaztelumendi, M.; Nazabal, J. Polymer 2001, 42, 9565.
40. Chiou, K. C.; Chang, F. C. J Polym Sci, Part B: Polym Phys 2000, 38, 23.